Chemical Data Collections 43 (2023) 100977

Contents lists available at ScienceDirect

Chemical Data Collections

journal homepage: www.elsevier.com/locate/cdc

Data Article

Synthesis, characterization of some substituted Quinolines derivatives: DFT, computational, *in silico* ADME, molecular docking and biological activities

Lynda Golea [a,*], Rachid Chebaki [b], Mohammed Laabassi [c], Paul Mosset [d]

[a] *Department of Material Sciences, Faculty of Science and Technology, Abbes Laghrour-Khenchela University, Khenchela 40000, Algeria*
[b] *Laboratory of Molecular Chemistry and Environment (LCME), Computer and Pharmaceutical Chemistry Team (ECIP), Faculty of Sciences and Exact Sciences. Department of Material Sciences, University of Biskra, BP 145 RP, Biskra 07000, Algeria*
[c] *Technical Science Department (ST), Batna-2 University, Algeria*
[d] *Rennes University, CNRS, ISCR (Institute of Chemical Sciences of Rennes), UMR 6226, Rennes F-35000, France*

ARTICLE INFO

Keywords:
Alcohols quinolines
Molecular docking
Antibacterial
Antioxidant
(ADME)

ABSTRACT

In the present work, an easy and conventional method has been adopted for the synthesis of novel quinoline alcohols in good yields. The structure of synthesized compounds was analysed by FTIR, ^{1} H, ^{13}C NMR. The prepared compounds were evaluated for antibacterial activity against one Gram-positive bacteria, and two Gram-negative bacteria. The result showed moderate antimicrobial activities. Also, antioxidant capacities of the synthesized compounds were determined by using DPPH method. Using DFT-based structure optimization, the HOMO-LUMO energy gaps of compounds (5a-c) were calculated theoretically at B3LYP in conjunction with the base 6-311G (d, p). Moreover, molecular docking studies were executed for the newly synthesized compounds to propose their mechanism of action against the coronavirus-2 (SARS-CoV-2) Protease Inhibitor. Of all compounds, quinoline derivatives shows the strongest affinity to ligand-receptor (PDB ID: 6LU7). *In silico* ADME study was also performed to predict the pharmacokinetic profile which expressed good oral drug-like behavior

Specifications Table *[please fill in right-hand column of the table below]*

Subject area	*Organic Chemistry*
Compounds	*Quinoline derivatives*
Data category	*Spectral data*
Data acquisition format	*FT-IR, (^{1}H and ^{13}C) NMR, DFT/B3LYP*
Data type	*Analyzed, synthesized*
Procedure	*The compounds were synthesized, characterized, and evaluated for antibacterial and antioxidant activities. Molecular docking studies were executed against the coronavirus-2 and In silico ADME study was also performed to predict the pharmacokinetic profile for the synthesized compounds.*
Data accessibility	*Data is within the article*

* Corresponding author.
E-mail address: golea.lynda@gmail.com (L. Golea).

https://doi.org/10.1016/j.cdc.2022.100977
Received 11 November 2022; Received in revised form 12 December 2022; Accepted 13 December 2022
Available online 15 December 2022

1. Rationale

Quinoline and its derivatives are gaining importance in medicinal and organic chemistry. They have displayed a broad spectrum of pharmacological and biological activities such as antimalarial [1, 2], anticancer [3, 4], antibacterial [5, 6], antifungal [7, 8], anti-diabetes [9], antivirals [10], antioxidants [11], anti-inflammatories [12], antiproliferatives [13], antitubercular [14] and corrosion inhibitors [15]. It is known, in the literature that the substituted quinolines, especially in positions C-2 and C-3, present very interesting biological activities such as anti-HIV-1 agents [16], and as inhibitors of SARS-CoV-2 [17]. In recent years the heterocyclic chemistry of quinolines is well established in the field of biological and pharmacological activities. This system has proved to be a very good scaffold for organic and medicinal chemists. However, quinoline derivatives were extensively studied as bioactive compounds, such as the quinoline alkaloids Quinine (1) that isolated from the bark of the Cinchona tree and has been used for the treatment of malaria [18]. Camptothecin (2) (Fig. 1), isolated from the Chinese tree Camptotheca acuminata, is the best known and most important quinoline alkaloid from an anticancer perspective [19]. Currently, quinoline alkaloids and their derivatives have very broad medical and agricultural applications.

In these reports we have designed and synthesized various C-2 and C-3 substituted quinoline derivatives from 2-chloroquinoline-3-carbaldehyde and evaluated their antibacterial, and radical scavenging activities have been investigated by using DPPH method. All the synthesized compounds exhibited moderate antibacterial and antioxidant activities. Due to the therapeutic properties of these derivatives, characterization of structural, geometrical and electronic properties by DFT calculations is fundamental to find out the influence of different substituents on the pharmacological properties of these quinoline rings. In this present work, a simulated molecular docking study of synthesized compounds was studied on the SARS-CoV2 enzyme to determine the types of amino acids responsible for the reaction at the level of the bonds formed with ligand-protien in the three-dimensional structure. Drugs like chloroquine (CQ), hydroxychloroquine (HCQ) are used as promising agents against COVID-19. Additionally, *in silico* ADME analysis was studied for molecules to check drug ability and toxicity issues. Our hypothesis is to study these synthesized products which contain the quinoline nucleus to determine the binding affinities of these drugs and to identify the main amino acid residues which play a key role in their mechanism of action by utilization of molecular docking which is a very useful strategy for optimizing the best virtual drug assays in the fastest and least expensive manner. According to published works, we have prepared some 2-chloro-3-dimethxymethyl-quinoline derivatives (2a-c). The substitution of chlorine in position C-2 by nucleophilic agent requires the protection of the aldehydic function in the form of acetal to avoid any attack on carbonyl site. The reagent used for this protection is the trimethoxy methane in methanol refluxed during 8 hours. After the protection of the aldehydic function in the first step, we carried out the substitution of chlorine in position C-2. We have reacted allyl alcohol in the presence of the hydride of sodium in the DMF with 2-chloro-3-dimethoxymethyl-quinoline to lead to ethers (3a-c) with good yields. Deprotection of the aldehyde function requires a quantity of para-toluenesulphonic acid and a water/THF mixture to lead to the compounds (4a-c). When we treated derivatives of compound (4a-c) with methyl magnesium iodide in dry THF at room temperature, we obtained products (5a-c) of (80%) yield. The structures of synthesized compounds were confirmed by FT-IR, ^{1} H NMR and ^{13}C NMR and theoretical calculations. The general synthetic of title compounds is shown (Scheme 1).

2. Procedure

2.1. Chemistry

All Chemical reagents and solvents were used as received and without any purification. Reactions were examined with TLC using silica gel 60 F254 from Merck. Melting points were measured using Electrothermal capillary fine control apparatus and are uncorrected. The FT-IR spectrum was recorded with JASCO FT/IR-4100 FT-IR spectrometer over the range 400-4000 cm^{-1}. ^{1}H and ^{13}C NMR spectra were recorded in DMSO-d_6 solutions on a Fourrier ARX 400 spectrometer at 400 MHz.

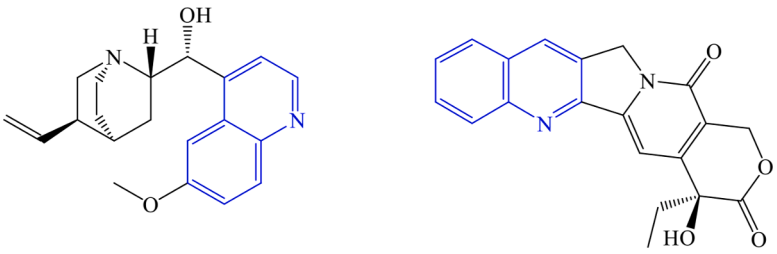

(1) (2)

Fig. 1. Molecular structures of quinoline alkaloids quinine (1) and Camptothecin (2)

2.1.1. Preparation of 2-chloro-3-formyl-quinoline

2-chloro-3-formylquinoline derivatives 1 have been synthesized according to the literature procedures [20]. Spectroscopic results and physical properties are in full agreement with literature reports [21].

2.1.2. Protection of the function aldehyde

General method: A solution of 1 (1g, 0.001 mmol) in 7 ml MeOH and (1 ml, 1.2 equiv.) of $CH(OCH_3)_3$ was refluxed during 8h. After cooling, the solution was extracted with CH_2Cl_2, washed with water, and dried with $MgSO_4$. Evaporation of solvent under reduced pressure gave the products 2, which were purified on silica gel column chromatography using petroleum ether/ethyl acetate: 9/1 as eluent.

-synthesis of 2-chloro-3-dimethoxymethyl-quinoline (2-a)

White crystals; yield = 81 %; mp = 61°C; IR n cm^{-1} (KBr): 3000-3010 (CH aromatics);

^1H NMR ($CDCl_3$) : 8.42 (s,1H, H-C_4), 8.03 (dd,1H, J = 8.5 Hz, J = 1.1 Hz, H-C_8), 7.87 (dd, 1H, J = 8.1 Hz, J = 1.4 Hz, H-C_5), 7.75 (ddd,1H, J = 8.5 Hz, J = 6.9 Hz, J =1.5 Hz, H–C_7), 7.58 (ddd,1H, J = 8.1 Hz, J = 6.9 Hz, J = 1.2 Hz, H–C_6), 5.73(d,1H, J = 0.6 Hz, CH $(OCH_3)_2$), 3.45 (s, 6H, $(OCH_3)_2$); ^{13}C NMR ($CDCl_3$): 149.00 (Cquat), 147.48 (Cquat), 137.28(CH), 130.90 (CH), 129.25 (Cquat), 128.25 (CH), 128.08 (CH), 127.26 (CH), 126.75 (Cquat), 100.40 (CH $(OCH_3)_2$), 53.90(CH $(OCH_3)_2$); HRMS m/z $[M]^{+\cdot}$ 273.0556 cald for $C_{12}H_{12}NO_2Cl$, found 237.0545.

-synthesis of 2-chloro-3-dimethoxymethyl-6-methyl-quinoline (2-b)

White crystals; yield = 94 %; mp = 64°C; IR n cm^{-1} (KBr): 3008-3001 (CH); ^1H NMR ($CDCl_3$): 8.32 (dd, 1H, J = 1.0 Hz, H-C_4), 7.92 (d, 1H, J = 8.6 Hz, H-C_8), 7.62-7.60 (m, 1H, H-C_5), 7.56 (dd, 1H, J = 8.6 Hz, J = 1.9 Hz, H-C_7), 5.73 (broad d, 1H, J = 1.0 Hz, CH $(OCH_3)_2$), 3.43 (s, 6H, $(OCH_3)_2$), 2.52 (s, 3H, CH_3); ^{13}C NMR ($CDCl_3$): 148.42 (C), 146.07(Cquat), 137.28 (Cquat), 136.60 (CH), 133.13 (CH), 129.12 (Cquat), 127.88 (CH), 126.90 (CH), 126.79 (Cquat), 100.51 (CH $(OCH_3)_2$), 53.88 (CH $(OCH_3)_2$), 21.59 (C_6-CH_3); HRMS m/z $[M]^{+\cdot}$ 251.1717 cald for $C_{13}H_{14}NO_2Cl$, found 251.0713.

-synthesis of 2-chloro-3-dimethoxymethyl-7-methoxy-quinoline (2-c)

White Crystals; yield = 94 %; mp = 64°C; IR n cm^{-1} (KBr): 3008-3001 (CH); ^1H NMR ($CDCl_3$) : 8.32 (dd, 1H, J = 1,0 Hz, H-C_4), 7.92 (d, 1H, J = 8.6 Hz, H-C_8), 7.62-7.60 (m, 1H, H-C_5), 7.56 (dd, 1H, J = 8,6 Hz, J = 1.9 Hz, H –C_7), 5.73 (broad d, 1H, J = 1.0 Hz, CH $(OCH_3)_2$), 3.43 (s, 6H, $(OCH_3)_2$), 2.52 (s, 3H, CH_3). ^{13}C NMR ($CDCl_3$): 148.42 (C), 146.07 (Cquat), 137.28 (Cquat), 136.60 (CH), 133.13 (CH), 129.12 (Cquat), 127.88 (CH), 126.90 (CH), 126.79 (Cquat), 100.51 (CH $(OCH_3)_2$), 53.88 (CH$(OCH_3)_2$), 21.59 (C_6-CH_3); HRMS m/z $[M]^{+\cdot}$ 251.1717 cald for $C_{13}H_{14}NO_2Cl$, found 251.0713.

2.1.3. Nucleophilic substitution

General method: A solution of hydride of sodium (0.5 g, 1.5 mmol) in the DMF (3 ml) was added 200 µl (1.2 equiv.) of R-OH at room temperature for 15 min, and then 2-chloro-3-dimethoxymethyl-quinoline 1 (0.5 g, 1.4 mmol) diluted in dry DMF (3 ml). The mixture was stirred for night. The solution was extracted with CH_2Cl_2, washed with water and dried with Na_2SO_4. Evaporation of solvent under reduced pressure gave the products 3 and 3', which were purified on silica gel column chromatography using petroleum ether/ethyl acetate: 8/2 as eluent.

-Preparation of 2-allyloxy-3-dimethoxymethyl-quinoline (3-a)

Yellow oil; yield = 85%; IR n cm^{-1} (KBr): 3012 (CH), 1597 (C=C); ^1H NMR ($CDCl_3$):8,25 (dd, 1H, J = 0.9 Hz, H-C_4), 7.82 (ddd, 1H, J = 8.4 Hz, J = 1.2 Hz, J = 0.6 Hz, H-C_8), 7.75 (ddd, 1H, J = 8.0 Hz, J = 1.5 Hz, J = 0.5 Hz, H-C_5), 7.61 (ddd, 1H, J = 8.4 Hz, J = 6.9 Hz, J = 1.5 Hz, H-C_7), 7.37(ddd, 1H, J = 8.0 Hz, J = 6.9 Hz, J = 1.2 Hz, H-C_6), 6.16 (ddt, 1H, J = 17.2 Hz, J = 10.5 Hz, J = 5.3 Hz, HC=CH_2), 5.70 (d, 1H, J = 0.7 Hz, H-C$(OMe)_2$), 5.46 (ddt, 1H, J = 17.2 Hz, J = 1.7 Hz, J = 1.7 Hz, HC=CH_2), 5.26 (ddt, 1H, J = 10.5 Hz, J = 1.5 Hz, J = 1.5 Hz, HC=CH_2), 5.07 (dt, 2H, J = 5.3 Hz, J = 1.5 Hz, OCH_2), 3.42 (s, 6H, CH$(OCH_3)_2$); ^{13}C NMR ($CDCl_3$): 159.00 (Cquat), 146.31(Cquat), 136.34 (CH), 133.54 (CH), 129.73 (CH), 127.96(CH), 126.90 (CH), 124.77 (Cquat), 124.19 (CH), 121.83 (Cquat), 117.18 (HC=CH_2), 98.95 (CH $(OCH_3)_2$), 66.58 (OCH_2), 53.74 (CH $(OCH_3)_2$). HRMS m/z [M^+ Na] $^+$: 282.1106 cald for $C_{15}H_{17}NO_3$, found 282.1106

-Preparation of 2-allyloxy-3-dimethoxymethyl-6-methy-quinoline (3-b)

Yellow Oil; yield = 88 %; IR n cm^{-1} (KBr): 3010 (CH), 1587 (C=C); ^1H NMR ($CDCl_3$): 8.14 (broed t, 1H, J = 1.0 Hz, H-C_4), 7.71 (d, 1H, J = 8.5 Hz, H-C_8), 7.53-7.50 (m,1H , H-C_5), 7 .44 (ddd, 1H, J = 8.5 Hz, J = 1.5 Hz, J = 0.6 Hz, H-C_7), 6.16 (ddt, 1H, J = 17.2 Hz, J = 10.5 Hz, J = 5.2 Hz, HC=CH_2), 5.69 (d, 1H, J = 0.7 Hz, H-C$(OMe)_2$), 5.45 (ddt, 1H, J = 17.2 Hz, J = 1.6 Hz, J = 1.6 Hz, HC=CH_2), 5.25 (ddt, 1H, J = 10.5 Hz, J = 1.5 Hz, J =1.5 Hz, HC=CH_2), 5.05 (dt, 2H, J = 5.3 Hz, J = 1.5 Hz, OCH_2), 3.42 (s, 6H , CH$(OCH_3)_2$), 2.47 (s, 3H, C_6-CH_3); ^{13}C NMR ($CDCl_3$): 158.64 (Cquat), 144.62 (Cquat), 135.80 (CH), 133.76 (Cquat), 133.65 (H-C=CH_2), 131.78 (CH), 127.06 (CH), 126.61 (CH), 124.73 (Cquat), 121.17 (Cquat), 117.06 (HC=CH_2), 99.04 (CH $(OCH_3)_2$), 66.48 (OCH_2), 53.74 (CH $(OCH_3)_2$), 21.30 (C_6-CH_3); HRMS m/z $[M]^{+\cdot}$: 273.1352 cald for $C_{16}H_{19}NO_3$, found 273.1364.

-Preparation of 2-allyloxy-3-dimethoxymethyl-7-methoxy-quinoline (3-c)

Yellow Oil; yield = 74 %; IR n cm^{-1} (KBr) : 3010 (CH), 1518(C = C); ^1H NMR ($CDCl_3$): 8.25 (broad s, H-C_4), 7.72 (d, 1H, J = 8.9 Hz, H-C_5), 7.24 (d ,1H , J = 2.5 Hz, H-C_8) , 7.18 (dd, 1H, J = 8.9 Hz, J = 2.5 Hz, H-C_6), 6.18 (ddt, 1H, J = 17.2 Hz, J = 10.5 Hz, J = 5.5 Hz, CH=CH_2), 5.69 (d, 1H, J = 0.5 Hz, H-C$(OMe)_2$), 5.50 (ddt, 1H, J = 17.2 Hz, J = 1.6 Hz, J = 1.6 Hz, HC=CH_2), 5.31 (ddt, 1H, J = 10.5 Hz, J = 1.3 Hz, J = 1.3 Hz, HC=CH_2), 5.07 (ddt, 2H, J = 5.3Hz, J = 1.6 Hz, J = 1.3 Hz, OCH_2), 3.93(s, 3H, C_7-OCH_3), 3.42 (s, 6H , CH $(OCH_3)_2$); ^{13}C NMR ($CDCl_3$): 160.47 (Cquat), 149.21 (Cquat), 147.63 (Cquat), 135.45 (CH), 132.77 (H-C=CH_2), 129.79 (CH), 124.80 (Cquat), 121.40 (Cquat), 117.93 (HC=CH_2), 117.86 (CH), 106.38 (CH), 100.47 (CH $(OCH_3)_2$), 66.88 (OCH_2), 55.68 (C_7-OCH_3), 53.90 (CH $(OCH_3)_2$); HRMS m/z $[M]^{+\cdot}$ 289.1312 cald for $C_{16}H_{19}NO_4$, found 289.1314.

2.1.4. Hydrolysis (obtaining aldehyde)

General method: a solution of compounds 3 (1g, 0.36 mmol) in the THF (2.65 ml), (9.25 ml) of water and (62 mg, 0.36 mmol, 0.1 equiv.) of APTH, was refluxed during 2 h. After cooling the solution was extracted with CH_2Cl_2, washed with water and dried with Na_2SO_4. Evaporation of the solvent under reduced pressure gave the products 4, which were isolated by column chromatography using petroleum ether/ethyl acetate: 8/2 as eluent.

-Preparation of 2-allyloxy-3-formyl-quinoline (4-a)

White crystals; yield = 69 %; mp = 68°C; IR n cm $^{-1}$ (KBr) : 3015 (CH), 1696 (C=O), 1607 (C=C); ^{1}H NMR ($CDCl_3$): 0.52 (s, 1H, C<u>H</u>O), 8.61 (broad s, 1H, <u>H</u>-C_4), 7.87-7.83(m, 2H, <u>H</u>-C_8, and <u>H</u>-C_5), 7.73(ddd, 1H, J = 8.5 Hz, J = 6.9 Hz, J = 1.4 Hz, <u>H</u>-C_7), 7.43(ddd, 1H, J = 8.0 Hz, J = 6.9 Hz, J = 1.2 Hz, <u>H</u>-C_6), 6.20 (ddt, 1H, J = 17.2 Hz, J = 10.5 Hz, J = 5.5 Hz, <u>H</u>C=CH_2), 5.49 (ddt, 1H, J = 17.2 Hz, J =1.6 Hz, J =1.6 Hz, HC=C<u>H</u>$_2$), 5.33 (ddt, 1H , J = 10.5 Hz, J = 1.6 Hz, J = 1.4 Hz, HC=C<u>H</u>$_2$), 5,13 (dt, 2H, J = 5.5 Hz, J = 1.4 Hz, OC<u>H</u>$_2$). ^{13}C NMR ($CDCl_3$): 189.27 (<u>C</u>HO), 160.53 (Cquat), 148.91 (Cquat), 139.92 (CH), 132.93 (H-<u>C</u>=CH_2), 132.58 (CH), 129.76(CH), 127.30 (CH), 125.09 (CH), 124.43 (Cquat), 119.99 (Cquat), 118.07 (H-C= <u>C</u>H$_2$), 67.08 (O<u>C</u>H$_2$); HRMS m/z [M]$^{+\cdot}$: 213.0789 cald for $C_{13}H_{11}NO_2$, found 213.0789.

-Preparation of 2-allyloxy-6-methyl-3-formyl-quinoline (4-b)

Green Crystals; yield = 80 %; mp = 89°C; IR n cm $^{-1}$ (KBr) : 3012 (CH), 1694 (C=O), 1565 (C=C); ^{1}H NMR ($CDCl_3$): 10.51 (s,1H, C<u>H</u>O), 8.52 (broad s, 1H, <u>H</u>-C_4), 7.74 (d, 1H, J = 8.5 Hz, <u>H</u>-C_8), 7,60-7.61 (m, 1H, <u>H</u>-C_5), 7.56 (dd, 1H , J = 8.5 Hz, J = 2.0 Hz, <u>H</u>-C_7), 6.19 (ddt, 1H, J = 17.2 Hz, J = 10.5 Hz, J = 5.5 Hz, <u>H</u>C=CH_2), 5,49 (ddt, 1H, J = 17.2 Hz, J = 1.5 Hz, J = 1.5 Hz, HC=C<u>H</u>$_2$), 5.32 (ddt, 1H , J = 10.5 Hz, J = 1.4 Hz, J =1.4 Hz, HC=C<u>H</u>$_2$), 5.11 (dt, 2H, J = 5.5 Hz, J = 1,4 Hz, OC<u>H</u>$_2$), 2.50 (s, 3H, C_6-C<u>H</u>$_3$); ^{13}C NMR ($CDCl_3$): 189.40 (<u>C</u>HO), 160.18 (Cquat), 147,32 (Cquat), 139.29 (CH), 134.85 (Cquat), 134.80 (H-<u>C</u>=CH_2), 133.05 (CH), 128.62 (CH), 126.99 (CH), 124.41 (Cquat), 120.00 (Cquat), 117.93 (H-C= <u>C</u>H$_2$), 66.98 (O<u>C</u>H$_2$), 21.24 (C_6-<u>C</u>H$_3$); HRMS m/z [M]$^{+\cdot}$: 227.0946 cald for $C_{14}H_{13}NO_2$, found 227.0955.

-Preparation of 2-allyloxy-7-methoxy-3-formyl-quinoline (4-c)

White crystals; yield = 74 %; mp = 94°C; IR n cm $^{-1}$ (KBr): 3008 (CH), 1689 (C=O), 1524 (C=C); ^{1}H NMR ($CDCl_3$): 10.47 (s, 1H, C<u>H</u>O), 8.61 (broad dd, 1H, J = 0.5 Hz, <u>H</u>-C_4), 7.72 (d, 1H, J = 8.9 Hz, <u>H</u>-C_5), 7.20 (broad d, 1H, J = 2.5 Hz, <u>H</u>-C_8), 7.06 (dd, 1H, J = 8.9 Hz, J = 2.5 Hz, <u>H</u>-C_6), 6.20 (ddt, 1H, J = 17.2 Hz, J = 10.5 Hz, J = 5.5 Hz, <u>H</u>-C=CH_2), 5.49 (ddt, 1H, J = 17.2 Hz, J = 1.6 Hz, J =1,6 Hz, HC=C<u>H</u>$_2$), 5.33 (ddt, 1H, J = 10.5 Hz, J = 1.6 Hz, J = 1.3 Hz, HC=C<u>H</u>$_2$), 5.11 (ddd, 2H, J = 5.5 Hz, J = 1.6 Hz, J = 1.4 Hz,OC<u>H</u>$_2$), 3.97 (s, 3H, OC<u>H</u>$_3$); ^{13}C NMR ($CDCl_3$): 189.05 (<u>C</u>HO), 163,60 (Cquat), 161.35 (Cquat), 151.31 (Cquat), 139.34 (CH), 132.99 (H-<u>C</u>=CH_2), 130.94 (CH), 119.35 (Cquat), 117.93 (H-C=<u>C</u>H$_2$), 117.89 (CH), 117.70 (Cquat), 106.27 (CH), 67.00 (O<u>C</u>H$_2$), 55.68(C_7,O<u>C</u>H$_3$); HRMS m/z [M]$^{+\cdot}$: 243.0895 cald for $C_{14}H_{13}NO_3$, found 243.08954.

2.1.5. Alkylation

General method: A solution of 4 (1g, 0.23 mmol) in dry THF (25 ml) was cooled at 0°C, we added CH_3MgI (6.5 ml, 2.5 equiv.) dropwise. The reaction mixture was stirred at room temperature for 2 h. HCl (1.3 N) was added slowly at 0°C. The solution was extracted with CH_2Cl_2, washed with water, and dried with Na_2SO_4. Evaporation of the solvent under reduced pressure gave the products 5, which were isolated by column chromatography using petroleum ether/ethyl acetate: 7/3 as eluent.

-Preparation of 1-(2-allyloxy-quinolin-3-yl)-ethanol (5-a)

White crystals; yield = 90 %; mp = 74°C; IR n cm $^{-1}$ (KBr): 3241 (OH), 3005 (CH); 1639 (C=C); ^{1}H NMR ($CDCl_3$): 8.03 (t, 1H, J = 0.9 Hz, <u>H</u>-C_4), 7.82 (ddd, 1H, J = 8.4 Hz, J = 1.1 Hz, J = 0.6 Hz, <u>H</u>-C_8), 7.73 (dd, 1H , J = 8.0 Hz, J = 1.5 Hz, <u>H</u>-C_5), 7 .60 (ddd, 1H, J = 8.4 Hz, J = 7.0 Hz, J = 1.5 Hz, <u>H</u>-C_7), 7.38 (ddd, 1H, J = 8.0 Hz, J = 7.0 Hz, J = 1.2 Hz, <u>H</u>-C_6), 6.17 (ddt, 1H, J = 17.2 Hz, J = 10.5 Hz, J = 5.5 Hz, <u>H</u>C=CH_2), 5.45 (ddt, 1H, J = 17.2 Hz, J = 1.6 Hz, J = 1.6 Hz, HC=C<u>H</u>$_2$), 5.29 (ddt, 1H , J = 10.5 Hz, J = 1.4 Hz, J = 1.4 Hz, HC=C<u>H</u>$_2$), 5.16 (broad q, 1H, J = 6.5 Hz, <u>H</u>-C(CH_3)OH), 5.07 (ddd, 2H, J = 5.5 Hz, J = 1.5 Hz, J = 1.5 Hz, OC<u>H</u>$_2$), 2.62 (broad s, 1H, O<u>H</u>), 1.60 (d, 3H, J = 6.5 Hz, HC(OH)-C<u>H</u>$_3$); ^{13}C NMR ($CDCl_3$): 158.89 (Cquat, <u>C</u>$_2$), 145.48 (Cquat), 133.93 (CH), 133.31 (H-<u>C</u>=CH_2), 129.20 (CH), 127.49(CH), 126,83 (CH), 125.34 (Cquat), 124.31 (CH), 117.69 (HC=C<u>H</u>$_2$), 66.71 (O<u>C</u>H$_2$). 66.07 (H<u>C</u>(CH_3) OH), 22.60 (HC(<u>C</u>H$_3$); MS: (M$^{\cdot+}$): 229.110 cald for $C_{14}H_{15}NO_2$, found 229.1092.

-Preparation of 1-(2-allyloxy-6-méthyl-quinolin-3-yl)-ethanol (5-b)

Yellow Crystals; yield = 85 %; mp = 76°C; IR n cm $^{-1}$ (KBr) : 3278 (OH); 3010 (CH); 1621 (C=C); ^{1}H NMR ($CDCl_3$): 7.94 (s,1H, <u>H</u>-C_4), 7.72(d, 1H, J = 8.5 Hz, <u>H</u>-C_8), 7.49-7.50(m, 1H, <u>H</u>-C_5), 7.43 (dd, 1H, J = 8.4 Hz, J = 1.9 Hz, <u>H</u>-C_7), 6.16 (ddt, 1H, J = 17.2 Hz, J = 10.5 Hz, J = 5.5 Hz, <u>H</u>C=CH_2), 5.44 (ddt, 1H, J = 17.2 Hz, J = 1.6 Hz, J = 1.6 Hz, HC=C<u>H</u>$_2$), 5.29 (ddt, 1H, J = 10.5 Hz, J = 1.3 Hz, J = 1.3 Hz, HC=C<u>H</u>$_2$), 5,14 (qd, 1H, J = 6.5 Hz, J = 0.7, <u>H</u>-C(CH_3)OH), 5.06 (ddd, 2H, J = 5.5 Hz, J = 1.4 Hz, J = 1.4 Hz, OC<u>H</u>$_2$), 2.42 (s, 3H, C_6-C<u>H</u>$_3$), 1.52 (d, 3H, J = 6.5 HZ, HC(OH)-C<u>H</u>$_3$); ^{13}C NMR ($CDCl_3$): 158.45 (Cquat), 143.68 (Cquat), 133.52 (CH), 131.36 (Cquat), 131.27 (H-<u>C</u>=CH_2), 131.27 (CH), 129.03(CH), 126.64 (CH), 126.47 (Cquat), 125.27 (Cquat), 117.62 (HC=C<u>H</u>$_2$), 66.70 (O<u>C</u>H$_2$), 66.14 (H<u>C</u>(CH_3)OH), 22.62 (HC(<u>C</u>H$_3$)OH), 21.33 (C_6-<u>C</u>H$_3$); HRMS m/z [M]$^{+\cdot}$: 243.1259 cald for $C_{15}H_{17}NO_2$, found 243.1265.

-Preparation of 1-(2-allyloxy-7-méthoxy-quinolin-3-yl)-ethanol (5-c)

White Crystals; yield = 84 %; mp = 76°C; IR n cm $^{-1}$ (KBr): 3271 (OH), 2999-3002 (CH), 1621 (C=C); ^{1}H NMR ($CDCl_3$): 8.03 (dd, 1H, J = 1.0 Hz, J = 0.9 Hz, <u>H</u>-C_4), 7.61 (d, 1H, J = 8.8 Hz, <u>H</u>-C_5), 7.20 (d, 1H, J = 2.5 Hz, <u>H</u>-C_8), 7.03 (dd, 1H, J = 8.8 Hz, J = 2.5 Hz, <u>H</u>-C_6), 6.17 (ddt, 1H, J = 17.2 Hz, J = 10.5 Hz, J = 5.5 Hz, <u>H</u>C=CH_2), 5.45 (ddt, 1H, J = 17.2 Hz, J = 1.6 Hz, J = 1,6 Hz, HC=C<u>H</u>$_2$), 5.30 (ddt, 1H, J = 10.5 Hz, J = 1.3 Hz, J = 1.3 Hz, HC=C<u>H</u>$_2$), 5.14 (qd, 1H, J = 6.5 Hz, J = 0.6 Hz, <u>H</u>-C(CH_3)OH), 5.06 (ddd, 2H, J = 5.5 Hz, J = 1.6 Hz, J = 1.3 Hz, OC<u>H</u>$_2$), 3.93 (s, 3H, C_7-OC<u>H</u>$_3$), 1.58 (d, 3H, J = 6.5 Hz, HC(OH)-C<u>H</u>$_3$); ^{13}C NMR ($CDCl_3$): 160.79 (Cquat), 159.44 (Cquat), 147.00 (Cquat), 133.82 (H-<u>C</u>=CH_2), 133.33 (CH), 128.50 (CH), 126.38 (Cquat), 120.02 (Cquat), 117.63 (H-C=<u>C</u>H$_2$), 116.48 (CH), 106.13 (CH), 66.65 (O<u>C</u>H$_2$), 66.00 (H<u>C</u>(CH_3)OH), 55.47 (C_7-O<u>C</u>H$_3$), 22.59 (HC(<u>C</u>H$_3$)OH); HRMS m/z [M]$^{+\cdot}$: 259.1208 cald for $C_{15}H_{17}NO_3$, found 259.1203.

2.2. Computational methods

The boundary orbitals are known as the highest occupied molecular orbitals (HOMO) and the lowest unoccupied molecular orbitals (LUMO), and these factors are very valuable for the chemical reactivity of any organic substance. While the HOMO orbital tends to lose electrons, the LUMO tends to receive them. The HOMO energy is related to the ionization potential while the LUMO energy is associated with the electronic activity. In this study, the HOMO-LUMO distributions, their energies in ev units, and their associated quantum chemical descriptors of compounds (5a-c) were investigated. The quantum chemical descriptors of these compounds have been calculated using the DFT/B3LYP method with the basis set 6-311+G (d, p) level of theory included within the Gaussian 09 package [22]. The (HOMO-LUMO energies, band gap energies, ionization potentials, electronic affinities, chemical hardnesses, softnesses and potentials, electronegativities, electrophilicity indices and maximum charge transfer indices) are calculated according to Koopman theorem [23] and Pearson and Parr [24, 25].

2.3. In vitro antibacterial activity

The compounds 5a, 5b and 5c were tested against three standard bacterial strains for the determination of their antibacterial activity, the results given in Table 1. All the compounds were screened for their antimicrobial activity against variety of bacterial strain such *Escherichia coli* ATCC 25922*, Staphylococcus aureus* ATCC 25923 and *Pseudomonas aeruginosa* ATCC 27853 using dimethyl sulfoxide (DMSO) as solvent and adjusted to a concentration of 250 and 500 μg/ml. The agar well diffusion method was used to determine antimicrobial activity [26]. The impregnated disks were placed on the medium suitably spaced apart and the plates were then incubated at 5°C for 1 hour to permit good diffusion and then were transferred to an incubator at 37°C for 24 hours for bacteria, the antibacterial activity was evaluated by measuring the inhibition zone diameter observed. Standard drugs like Ampicillin, Gentamycin were used for comparison purpose. The results were expressed as the mean of three measurements.

2.3. In vitro antioxydant activity

The radical scavenging activity of the synthesized compounds was evaluated with DPPH 1,1-diphenyl-2-picryl hydrazyl. Using the process [27], 20 mg/ml solution of DPPH in methanol was prepared daily. The synthesized samples in methanol to prepare six different concentrations (5, 15, 25, 30, 40 and 50 µg/ml), the mixtures were made by adding 1 ml of test sample to 1 ml of DPPH solution to 4 ml of methanol. Ascorbic acid was used for reference standard in similar concentration. The sotution mixtures were kept to stand for 30 min in dark oven at 37°C, and optical density was measured at 517 nm using the spectrophotometer. Percentage inhibition of DPPH radical was determined using the following equation:

Percent (%) inhibition of DPPH activity = 100 × (A' – B) /A'

Where A' = optical density of the blank and B = optical density of the sample

2.4. In silico molecular docking evaluation

In December 2019, the Corona virus disease (COVID-19) was identified in the Chinese city of Wuhan for the first time in the world [28]. After that, it began to spread rapidly around the world, costing the lives of millions of people. Chloroquine (CQ) and hydroxychloroquine (HCQ) are drugs used against SARS-CoV-2. These drugs can inhibit the viral protease, called chymotrypsin-like cysteine protease, also known as the Main protease (3CLpro); but unfortunately, there is no therapeutic effect against this virus. In this study we focused on the main protease of the virus COVID-19. As a potential target protein for treating the disease. The protiene 6LU7 is the main protease present in the corona virus, which was deposited as a PDB file in 2020 [29]. The mol2 file of active compounds (5a-c) were prepared using ChemBio3D Ultra 14.0. And the PDB formats of these compound were used over their optimized structures with B3LYP/6-311+G (d, p). All preparations for docking were carried out by Discover Studio Visualizer 2.5 software, and for the ligand and protein molecules, they were converted to file format (pdbqt) using AutoDock tools 1.5.6. Three-dimensional structures of the all drug targets were retrieved from the RCSB Protein Data Bank (PDB). Crystallographic structures of the COVID-19 M^{pro} (PDB ID: 6LU7) contsist of 2 chains, A and C, which may be part of interactions with the ligand.

Table 1
Calculated E HOMO, ELUMO, energy band gap (ΔE), electronegativity (ω), chemical potential (μ), global hardness (η), global softness (S), (in eV) using B3LYP/6-311+G (d, p).

Molécules	Total Energy	HOMO	LUMO	ΔE	μ	χ	S	ω	η
5a	-747,790	-6.36	-2.55	3.81	-4.45	4.45	0.26	5.19	1.90
5b	-787.115	-5.16	-2.51	2.65	-3.83	3.83	0.37	5.53	1.32
5c	-862,335	-6.14	-2.54	3.60	-4.34	4.34	0.27	5.23	1.80

2.5. In silico ADME studies

The prediction of the ADME (absorption, distribution, metabolism, excretion) before the experimental studies is one of the most important aspects of drug discovery and development processes. ADME studies play a significant role in helping to optimize the pharmacokinetic properties of new drugs [30]. The pharmacokinetic and Physicochemical properties of all compounds (5a-c) were determined by using SwissADME server (http://www.swissadme. ch/). The chemical structure of designed compounds is drawn by ChemDraw profssional 17.1 and then converted by SwissADME tool to SMILE name [31].

3. Results and discussion

3.1. Chemistry

This work has led us to establish a synthesis of new quinoline alcohols which are unknown in the literature, with the aim of leading to new active principles. In this work we proceeded to the synthesis of some derivatives of 2-chloro-3-formylquinoline derivatives (1a-c), one of which is unpublished, according to the method described by O. Meth-Cohn. [20]. The substitution of the chlorine atom in C-2 position of 2- chloro-3-formylquinoline derivatives by a nucleophile can be prevented by a parallel reaction between the nucleophile and the aldehyde function because of the very high reactivity of the latter. Therefore, we proceeded, in a first step, to the protection of the function to lead the compounds (2a-c). After the protection of the aldehyde function in the previous step, we reacted allyl alcohol in the presence of Sodium hydride in DMF with 2-chloro-3-formyl-quinoline derivatives to lead (3a-c). The next step requires the liberation of the aldehyde function in order to proceed to its alkylation, this leads us to deprotect the aldehyde function of the different quinolines, by heating them at reflux in a mixture of THF and distilled water for 1 hour in the presence of a catalytic amount of paratoluenesulfonic acid to lead to the expected ether aldehydes (4a-c). The ^{1}H NMR spectra allow us to observe the characteristics of the protons; A weak field singlet signal between 10.47 and 10.50 ppm corresponding to the proton of the carbon carrying the aldehyde function. The last step of this synthesis is to obtain the quinoline alcohols sought for their synthetic interest in organic chemistry. We proceeded to the alkylation of the aldehyde functions obtained in the previous step with methyl magnesium iodide in THF to lead to the expected (5a-c) in very good yields 85%. $^{1}H/^{13}C$ NMR spectra of compounds were investigated, and the resulting spectral data were given in the experimental section, In the ^{1}H NMR spectrum of the compounds (5a-c), the two protons of O-CH_2 appear between 5.06-5.08 ppm, however, the chemical shifts of the protons of the double bond Hcis, Htrans of HC=CH_2 have almost the same appearance in all cases between 5.40-5.49 ppm, and 5.28-5.30 ppm respetively, while the methoxyl groups resonate, as expected, around 4.00 ppm. But the methyl groups give a strong field singlet signal between 2.35-2.42 ppm. Again, the -CH- proton in the C-3 resonated as quadriplet doublet at δ 5.15 ppm. The doublet observed at δ 1.50 ppm is signal of protons of methyl group. The signals due to quinoline H-4 appeared as singlet between δ 7.94-8.03 for one proton, the signals due to quinoline H-5, H-6, H-7, H-8 appeared in the region δ 7.03-7.83. In the ^{13}C NMR spectrum of (5a-c), the signals of methyl groups (-CH_3) are seen at δ 23.86 ppm. The signal

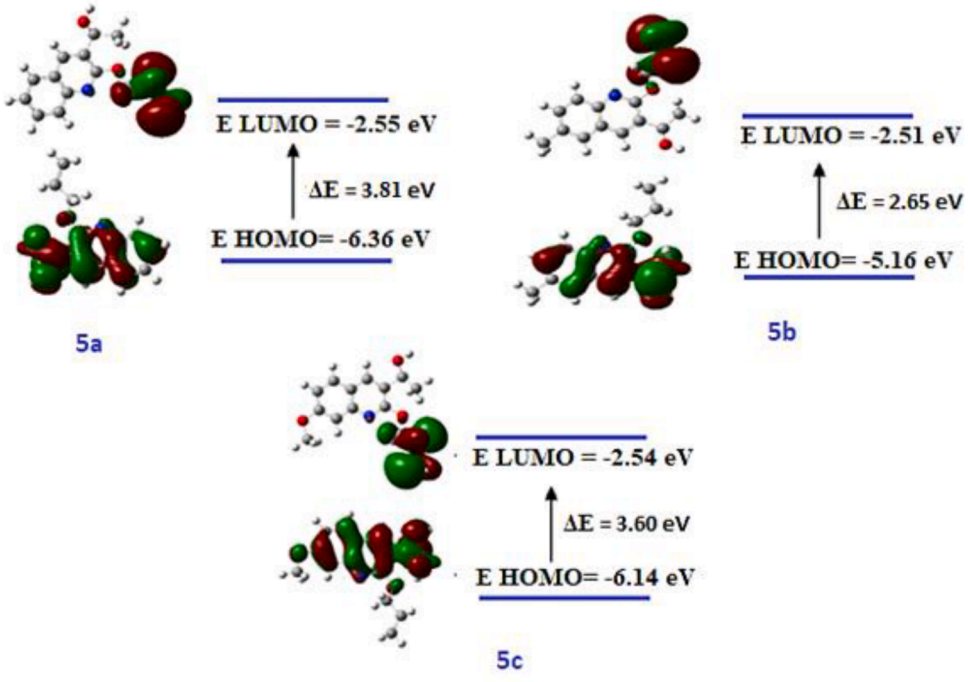

Fig. 2. The optimized structure, HOMO and LUMO of compounds (5a-c) obtained from density functional theory

observed at δ 22.50-22.60 ppm is the resonance signal of the -CH- carbon atom in C-3, that was observed between δ 66.00-66.10 ppm, and the signal belonging to the carbon atom ($O–CH_2$) was observed at δ 66.15 ppm. The signals of the aromatic carbon atoms and the carbon atom in the quinoline ring are observed in the range of δ 121.00-142.81 ppm. Spectroscopic data of all synthesized compounds are given in the experimental section. FTIR spectra of all compounds (5a-c) shows characteristic broad band at 3270-3273 cm^{-1} attributed to ν (-OH) indicating the presence of hydroxyl group. In line with these, the sharp peaks found in the FTIR at 3025 and 2930.9 cm^{-1} shows very strong asymmetric stretching vibrations of aromatic C-H and aliphatic C-H. The presence of nitrogen in the ring of benzene structure gives rise to C=N stretching vibrations at 1631-1625 cm^{-1}. The C-C aromatic stretching vibrations give rise to characteristic band in the IR spectra covering the spectral range from 1600-1582 cm^{-1}.

3.2. Frontier molecular orbital (FMO) analyses

The density functional theory is imposed as a relatively fast and efficient way to optimize the electronic and structural properties for all synthesized molecules or natural substances. In this work, we have presented the DFT theory and discussed mainly the essential points related to our project. The global reactivity parameters, associated to each molecule, have been calculated, in this case E Homo and E LUMO, E gap (ΔE), the chemical potential (μ), the electronegativity (χ), the index of electrophilicity (ω), chemical hardness (η) and softness (S) [32, 33]. The aim being to study the relationship and correlation between the structure of the synthesized molecules and the physicochemical and biological properties of these structures. The ground state molecular geometry of the (5a-c) were optimized by density functional theory (DFT/B3LYP) calculations and with the 6-311+G (d, p) basis set as implemented in the Gaussian 6 program package. The optimized geometry of molecules (5a-c) presented in (Fig. 2).

In HOMO (highest occupied molecular orbital) of compounds (5a-c), the electron density is strongly localized over quinoline moiety due to the presence of nitrogen and oxygen atoms as there is a presence of lone pair of electrons on them. The rest of the molecule appears to have neutral distribution of charge. In LUMO (lowest unoccupied molecular orbital) of same compounds the electron density is observed mainly on the C-2 allyloxy radical. The energy gap (ΔE) is observed to be 2.78 and 2.92 eV. The energy gap (ΔE) between the HOMO and LUMO orbitals is a critical parameter for the chemical reactivity and stability of structures. Generally, molecules with small energy gaps (ΔE) have low structural stability and high chemical reactivity. In contrast, molecules with large energy gaps have high structural stability and low chemical reactivity [34]. In our study, these parameters were calculated for the most active antioxidant compounds (5a-c). According to DFT calculations, energy bandgap values were found that 3.81, 2.65 and 3.60 eV for 5a, 5b end 5c respectively. From the values found, we can deduce that the compound 5a has much higher structural stability than the others, while the compound 5b has the lowest structural stability than the others. Likewise, we can conclude that the antioxidant activity increases as the energy band gap decrease. The computed values are tabulated in Table 1.

3.3. Molecular electrostatic potential analysis

Molecular electrostatic potential (MEP) analysis is very useful for estimating the reactive sites of electrophilically and nucleophilically attacked compounds [35]. MEP analysis at the B3LYP/6-31G + (d, p) is considered predictive of chemical reactivity since the regions of negative potential are expected to be the sites of protonation and nucleophilic attack, while the regions of positive potential may indicate the electrophilic sites on the entitled molecule. The obtained MEP were indicated as in Fig. 3. In this figure, there are three type colors on the MEP which are blue, green and red. Here blue color indicates the maximum positive which suitable locals for nucleophilic attack points, red represents maximum negative which suitable points for electrophilic attack, and green color indicates zero value in terms of electron density. In all compounds (5a-c) the red regions are localized over nitrogen of the quinoline moiety and oxygen of hydroxy group there by these sites are rich of electron and have affinity towards the electrophiles. The carbon and hydrogen atoms with blue and green colors are poor electron-deficient zones, which could attract nucleophilic moieties.

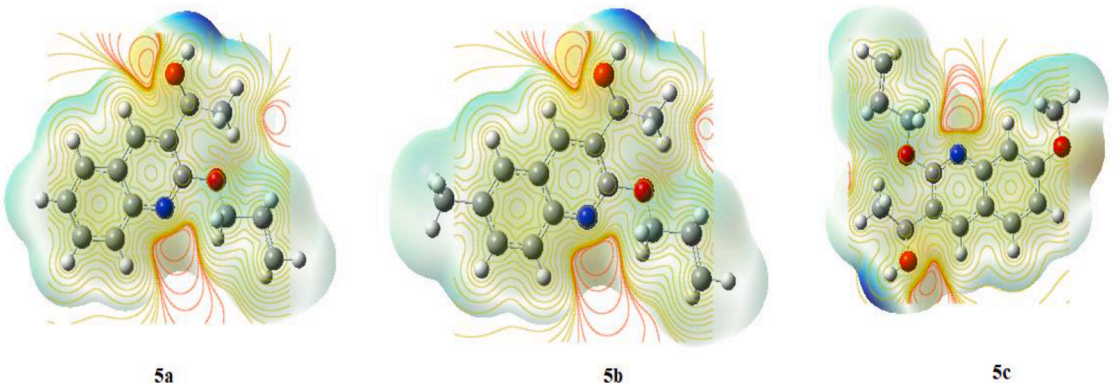

Fig. 3. The MEP surfaces of compounds (5a-c).

3.4. Antibacterial activity

In this work, an attempt was made to evaluate the newly compounds synthesized for their in vitro antibacterial activities against three bacterial pathogens including *S. aureus, E. coli*, and *P. aeruginosa* using paper disk diffusion method. Results demonstrated that the mean inhibition zone of the synthesized compounds varied from 9.33 to 15.1 mm. The mean inhibition zones displayed by the title compounds were different against all of the bacterial strains at 500 μg/ml (Table 2). Compound 5a and 5c showed mean inhibition zones against three of the bacterial strains. At the same concentration, the inhibition zone displayed by compound 5b against *P. aeruginosa* with a value of 11,667±1,527 mm. These newly synthesized compounds demonstrated moderate antimicrobial profile against all bacterial strains. Ampicillin and Gentamycin were used as standard antibacterial drugs respectively.

3.5. Antioxydant activity

The data in Fig. 4 reveal that all of the synthetic compounds showed moderate antioxidant activities with IC_{50} values between 327.67±1.28 and 434.46±1.91 μm, these values were nearly close to standard ascorbic acid with IC_{50} value 196.46±0.76 μm. The statistical analyze were performed by Microsoft Excel 2010 and all the numerical results were expressed graphically. The DPPH test measures the anti-free radical power of molecules, it measures the ability of an antioxidant to reduce the chemical radical DPPH (2,2-diphenyl-1-picrylhydrazyl) by transfer of hydrogen. The initially purple DPPH turns into pale yellow. This potential activity of these compounds can be explained by the presence of oxygen atoms. But in the compound 5c the presence of an ethoxy group that increases the activity of antioxidants and the degree of solubility of the substance in the aqueous medium and this is the formation of hydrogen bonds, which stabilizes the radicals and improves the antioxidant properties *in vitro*.

2.4. In silico molecular docking evaluation

Molecular docking is a very important way of understanding the binding interactions between a ligand and a protein receptor. This method for drug design is exceptionally reliable, time-saving and cost-effective. The (5a-c) compounds containing quinoline cycle, and these types of molecules have profound medicinal and pharmacological importance, so we have undertaken in silico based molecular docking study. Initially, we optimized the ligand molecules with the B3LYP/6-311 G + (d, p) level of theory, and the optimized structures were used for docking analysis. We obtained target main protease ($3CL^{pro}$) of SARS-CoV-2 (PDB ID: 6LU7). This target protein structure was taken from the Protein Data Bank [29]. The water molecules and ligands in the target structure were removed. Both ligand and target structures were prepared with AutoDock tools 1.5.6. The best binding pose for each compound was predicted using the discovery studio program, as shown in Fig. 5, Fig. 6 and Fig. 7. The docking score (in kcal/mol) for (5a-c) are -6.18, -5.96 and -6.07 respectively. The binding score suggests that all compounds display similar binding affinity against SARS-CoV-2. The binding energies of all docked conformations for the title compounds (5a-c) and CQ, HCQ are presented in Table 3. Therefore, in the present work, the molecular docking analysis of the synthesized compounds (5a-c) was carried out to investigate their binding pattern with target ($3CL^{pro}$) having PDB ID 6LU7 and compare them with standard antimalarial drugs chloroquine (CQ) and its hydroxychloroquine (HCQ) are currently used as drugs for the treatment of COVID-19 [36]. The synthesized compounds (5a-c) showed similar residual interactions profile with amino acid residues His163, Cys145, Met165 and His41. Compounds 5b and 5c have additional hydrogen bonding interaction with amino acid residue Cys 145.

2.5. In silico ADME

SwissADME webserver was used to measure the bioactivity score of the synthesized compounds (5a-c). The calculated pharmacokinetics and physicochemical parameters such as cLogP (partition coefficient), compound weight, heavy atoms, hydrogen donors, hydrogen acceptors, rotatable bonds and TPSA values are illustrated in Table 4. From this table, the novel compounds (5a-c) exhibit no Lipinski's violation and having 1 hydrogen bond donors and 3-4 hydrogen bond acceptors. In addition to that, the molecular weight of the synthesized compounds (5a-c) is not more than 500 m/z. As per the above-mentioned parameters, the title compounds have good drug-likeness profile and the compound 5c reveals excellent drug-likeness criteria. The compounds 5a and 5b show 4 rotatable bonds but the compounds 5c exhibit 5 rotatable bonds. This reveals that, the title compounds have excellent ability to interact with the living cells. The bioavailability is the important parameter and the values of bioactivity score greater than zero indicates excellent drug

Table 2
Antimicrobial screening data of compounds (5a-c).

Compounds	Compound 5a		Compound 5b		Compound 5c		AMP	GEN
Concentration	500 μg/ml	250 μg/ml	500 μg/ml	250 μg/ml	500 μg/ml	250 μg/ml	10 μg/disc	10 μg/disc
E.coli	10,333±0,577	7,000±2,000	9,333±1,528	6,667±1,155	14,667±0,577	12,000±1,000	28	32
S.aureus	14,333±1,527	11,333±2,081	10,667±0,577	8,667±1,155	13,667±1,527	10,333±1,527	14	15
P.aurengenosa	10,667±1,527	10,333±1,527	11,667±1,527	9,000±2,000	15,100±2,000	12,000±1,000	19	20

zone of inhibition in mm: < 10: week; > 10: moderate; >16: Significant
AMP: Ampicillin
GEN: Gentamycin

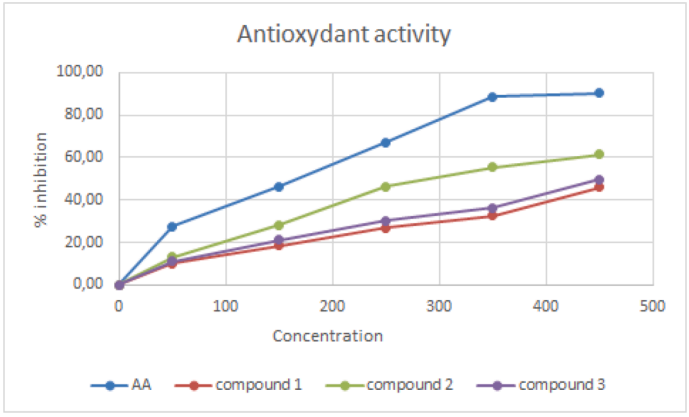

Fig. 4. Antioxydant activity results using DPPH by the synthetic compounds.

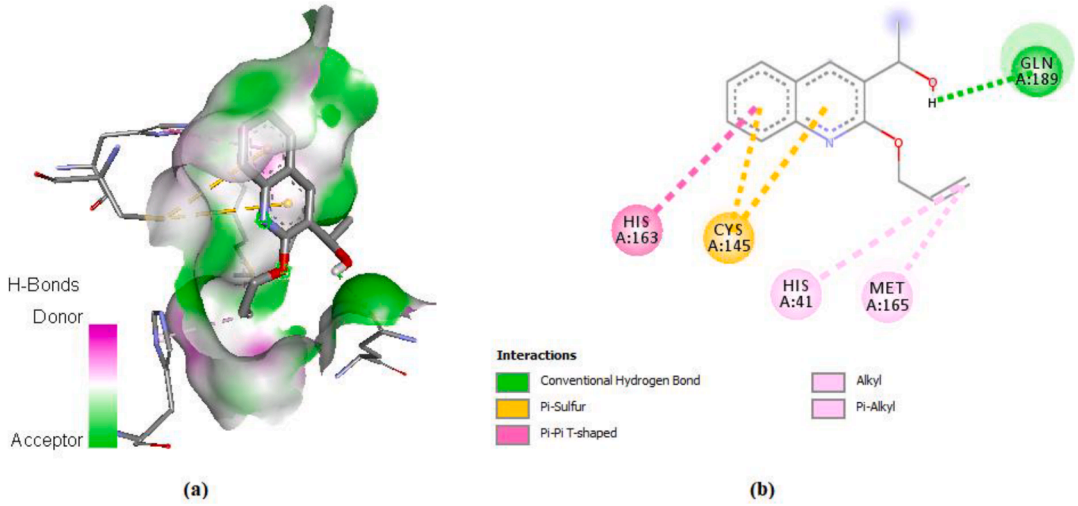

Fig. 5. (a) 3D and (b) 2D molecular docking results of the compound (5a) + 6LU7.

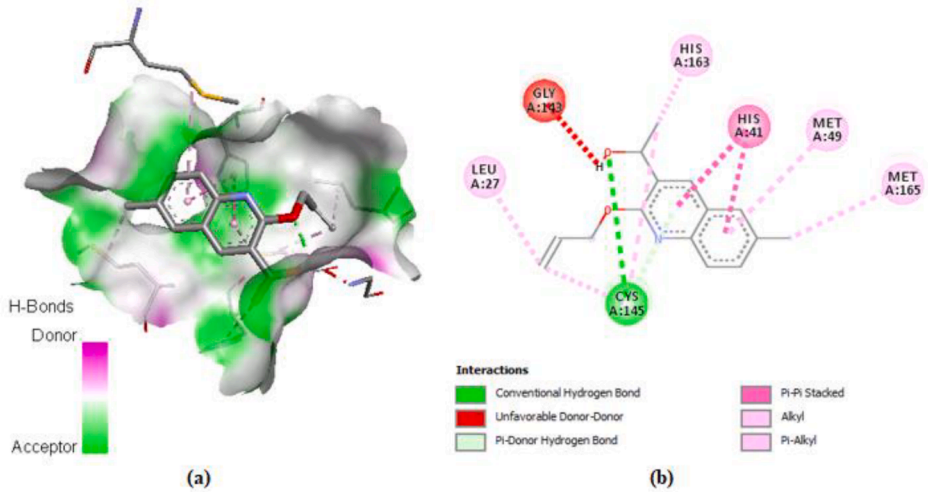

Fig. 6. (a) 3D and (b) 2D molecular docking results of the compound (5b) + 6LU7.

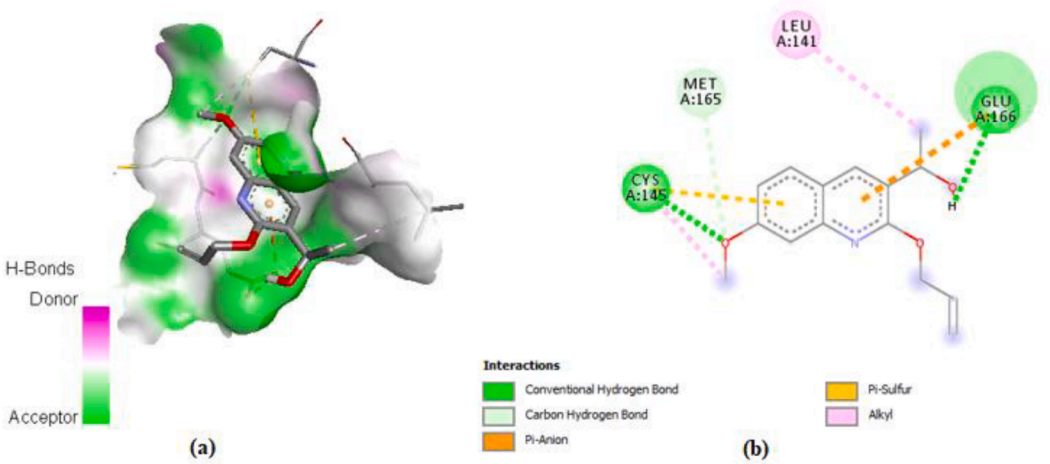

Fig. 7. (a) 3D and (b) 2D molecular docking results of the compound (5c) + 6LU7.

Table 3
xxx

Lig name	Binding energy (kcal/mol)	Hydrogen bond	Hydrophobic and other Interactions
5a	-6.18	Gln143	His163, Cys145, His41, Met165
5b	-5.96	Cys 145	Gly143, His163, Leu27, His41, Met 49, Met 165,
5c	-6.07	Glu 166, Cys 145	His163, Leu 141, Met 165
CQ	-6.13[37]	Gly143, Cys145, His164	His41, Asn142, His163
HCQ	-6.58[37]	Phe140, Asn142, Ser144, Glu166	Phe140, Asn142, Cys145, Glu166, His172

Table 4
Calculated *in silico* ADME parameters of the synthesized quinoline derivatives (5a-c).

Compounds	MW[a] (≤500)	TPSA[b] (A2)	HBA[c] (≤10)	HBD [d] (≤5)	RB[e] (≤5)	cLogP[f] (≤5)	Bioavailability Score	Lipinski's Violation
5a	229.27	42.35	3	1	4	2.62	0.55	0
5c	243.30	42.35	3	1	4	2.97	0.55	0
5d	259.30	51.58	4	1	5	2.64	0.55	0

[a] Molecular weight.
[b] Topological polar surface area.
[c] Number of hydrogen bond acceptor.
[d] Number of hydrogen bond donor.
[e] Number of rotatable bonds.
[f] Consensus of calculated lipophilicity.

likeness of the molecule [38]. All the new quinoline derivatives (5a-c) have the bioactivity scores of 0.55 (Fig. 8.A).

Pharmacokinetically, all synthesized compounds (5a-c) have high GI absorption, blood brain barrier (BBB) propertie, and medium skin permeation value, and none of the synthesized compounds were predicted as P-glycoprotein substrate. Pharmacokinetically measurements give significant information about the permeation ability of the synthesized compounds (5a-c) which were determined using BOILED-Egg method and the graph is represented in (Fig. 8.B). Points located in the BOILED-Egg's yolk (yellow) signify the molecules predicted to passively permeate through the blood-brain barrier (BBB) whereas The red ones point out to the molecules predicted not to be effluated from the CNS (Central Nervous System- by the P-glycoprotein). However, the ones in the egg white are relative to the molecules predicted to be passively absorbed by the gastrointestinal tract.

Conclusion

In this study, we reported an easily applicable and efficient method for the synthesis of quinoline derivatives (5a-c) by application of Vilsmeier-Haack reaction. Various nucleophiles were introduced into 2-chloroquinoline-3-carbaldehyde using different reaction

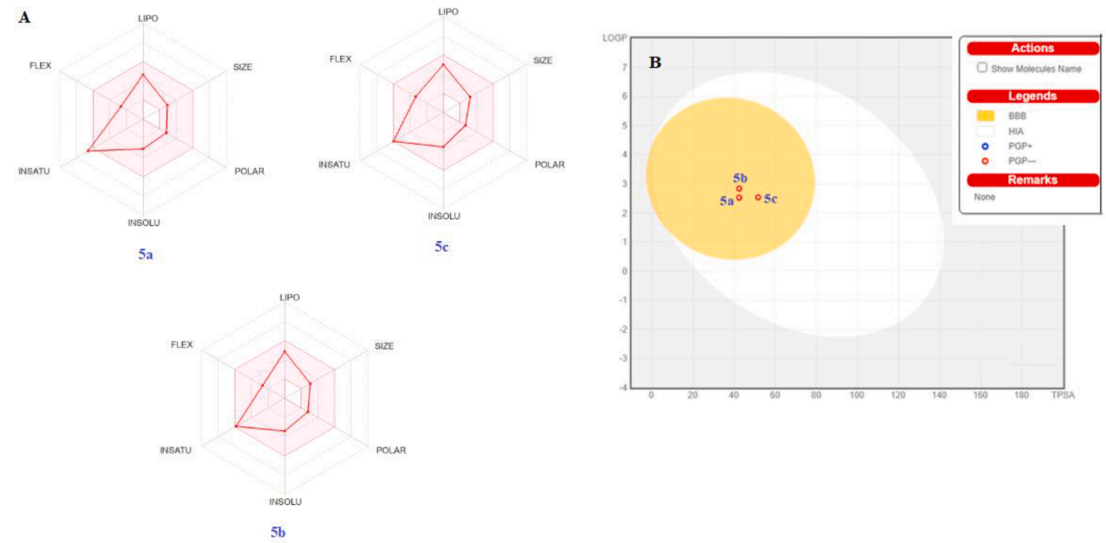

Fig. 8. (A) Bioavailability radar and (B) the BOILED-Egg model of synthesized molecules (5a-c).

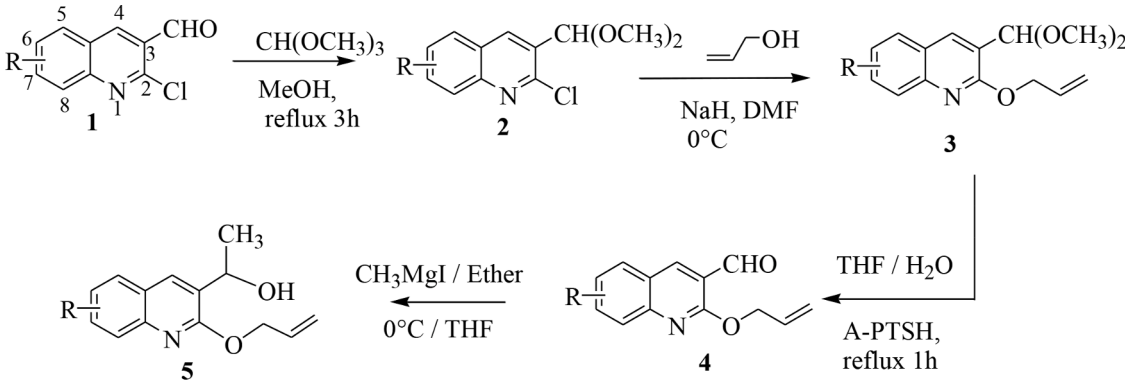

R: a = H, b = 6-Me, c = 7-OMe

Scheme 1. Synthesis of compounds (5a-c).

and conditions to lead C-2 and C-3 substituted quinoline. The structure and purity of all the compounds were indicated by their spectral and physical data. The antibacterial activities of the synthesized compounds were screened by the disc-diffusion method against one Gram-positive and two Gram-negative bacteria. Most of them were found to have moderate activities against the all bacterial strains. In the Gaussian calculations made, the chemical activity of the molecules (5a-c) was highest in the calculations made in the 6-311G (d, p) basis set. The *In silico* molecular docking study of the synthesized compounds (5a-c) was performed to assess the binding mode of these compounds against the coronavirus-2 (SARS-CoV-2) Protease Inhibitor (PDB ID : 6LU7). The three compounds (5a-c) exhibited good affinity with the coronavirus-2 (SARS-CoV-2). The ADME prediction has been shown a promising result *in silico* properties which indicate that all the synthesized compounds have an improved pharmacokinetic profile.

CRediT authership contribution statement

Lynda Golea: Synthesis, Spectroscopic characterizations, Molecular docking, DFT calculations, Methodology, Visualization, Writing-original draft. **Rachid Chebaki:** Molecular docking, Visualization, Software. **Mohammed Laabassi:** Spectroscopic characterizations, Methodology, Investigation. **Paul Mosset:** Spectroscopic measurements.

Declaration of Competing Interest

The authors declare that they have no known competing financial interests or personal relationships that could have appeared to influence the work reported in this paper.

Data availability

No data was used for the research described in the article.

Acknowledgments

The synthesis part of this work was carried out at the Laboratory of Chemistry and Chemistry of the Environment (L.C.C.E), Department of Chemistry, Faculty of Materials Sciences, University of Batna-1, Batna. The authors would like to thank all the members of the laboratory (L.C.C.E) for the help provided, either products or materials. And we also thank the Algerian MESRS (Ministère de l'Enseignement Supérieur et de la Recherche Scientifique). And all the people who helped to carry out this work such as biological activities and theoretical studies.

Supplementary materials

Supplementary material associated with this article can be found, in the online version, at doi:10.1016/j.cdc.2022.100977.

References

[1] A. Kumar, K. Srivastava, S.R. Kumar, S.K. Puri, P.M.S. Chauhan, Synthesis and bioevaluation of hybrid 4-aminoquinoline triazines as a new class of antimalarial agents, Bioorg. Med. Chem. Lett. 18 (2008) 6530–6533.
[2] Z. Xu, C. Gao, Q.C. Ren, X.F. Song, L.S. Feng, Z.S. Lv, Recent advances of pyrazole-containing derivatives as anti-tubercular agents, Eur. J. Med. Chem. 139 (2017) 429–440.
[3] O. Afzal, S. Kumar, M.R. Haider, M.R. Ali, R. Kumar, M. Jaggi, S. Bawa, A review on anticancer potential of bioactive heterocycle quinoline, Eur. J. Med. Chem. 97 (2015) 871–910.
[4] S. Jain, V. Chandra, P.K. Jain, K. Pathak, D. Pathak, A. Vaidya, Comprehensive review on current developments of quinoline-based anticancer agents, Arab. J. Chem. 12 (2019) 4920–4946.
[5] N. Sun, R.L. Du, Y.Y. Zheng, B.H. Huang, Q. Guo, R.F. Zhang, K.Y. Wong, Y.J. Lu, Antibacterial activity of N-methylbenzofuro[3,2-b] quinoline and N-methylbenzoindolo[3,2-b]-quinoline derivatives and study of their mode of action, Eur. J. Med. Chem. 135 (2017) 1–11.
[6] M.F. El Shehry, M.M. Ghorab, S.Y. Abbas, E.A. Fayed, S.A. Shedid, Y.A. Ammar, Quinoline derivatives bearing pyrazole moiety : synthesis and biological evaluation as possible antibacterial and antifungal agents, Eur. J. Med. Chem. 143 (2018) 1463–1473.
[7] D. Ben Yaakov, Y. Shadkchan, N. Albert, D.P. Kontoyiannis, N. Osherov, The quinoline bromoquinol exhibits broad-spectrum antifungal activity and induces oxidative stress and apoptosis in Aspergillus fumigatus, J. Antimicrob. Chemother. 72 (2017) 2263–2272.
[8] R. Musiol, J. Jampilek, V. Buchta, L. Silva, H. Niedbala, B. Podeszwa, A. Palka, K. Majerz-Maniecka, B. Oleksyn, J. Polanski, Antifungal properties of new series of quinoline derivatives, Bioorg. Med. Chem. 14 (2006) 3592–3598.
[9] D. Edmont, R. Rocher, C. Plisson, J. Chenault, Synthesis and evaluation of quinoline carboxyguanidines as antidiabetic agents, Bioorg. Med. Chem. Lett. 10 (2000) 1831–1834.
[10] N. Mahmoudi, L. Ciceron, J.F. Franetich, K. Farhati, O. Silvie, W. Eling, R. Sauerwein, M. Danis, D. Mazier, F. Derouin, In vitro activities of 25 quinolones and fluoroquinolones against liver and blood stage Plasmodium spp, Antimicrob. Agents Chemother 47 (2003) 2636–2639.
[11] L. Savegnago, A.I. Vieira, N. Seus, B.S. Goldani, M.R. Castro, E.J. Lenardão, D. Alves, Synthesis and antioxidant properties of novel quinoline–chalcogenium compounds, Tetrahedron Lett. 54 (2013) 40–44.
[12] Yeh-L. Chen, I-Li. Chen, Chih-M. Lu, Cherng-Ch. Tzeng, Lo-T. Tsao, Jih-P. Wang, Synthesis and anti-inflammatory evaluation of 4-anilinofuro[2,3-b] quinoline and 4-phenoxyfuro[2,3-b] quinoline derivatives. Part 3, Bioorg Med Chem 15 (2004) 387–392.
[13] P.V. Joshi, A.A. Sayed, A. RaviKumar, V.G. Puranik, S.S. Zinjarde, 4-Phenyl quinoline derivatives as potential serotonin receptor ligands with antiproliferative activity, Eur. J. Med. Chem. 136 (2017) 246–258.
[14] A. F.Borsoi, L.M. Alice, N. Sperotto, A.S. Ramos, B.L. Abbadi, F.S. Macchi, A.S. Dadda, R.S. Rambo, R.B.M. Silva, J.D. Paz, K. Pissinate, M.N. Muniz, C.E. Neves, L. Galina, L.C. González, M.A. Perelló, A.M. Czeczot, M. Leyserd, S.D. Oliveirac, G. Araújo Locke, B.V. de Araújoe, T.D. Costa, C.V. Bizarro, L.A. Basso, Pablo Machado, Antitubercular activity of novel 2-(quinoline-4-yloxy) acetamides with improved drug-like properties, ACS Med Chem Lett 13 (2022) 1337–1344.
[15] F. Zhong, G. Geng, B. Chen, T. Pan, Q. Zhang, H. Li, C. Bai, Identification of benzenesulfonamide quinoline derivatives as potent HIV-1 replication inhibitors targeting Rev protein, Org. Biomol. Chem. 13 (2015) 1792–1799.
[16] S. Purvi, N. Dharav, J. Nisha, B. Deepali, K. Sanjay, K. Smita, K.B. Kamlesh, P.S Inder, Synthesis of C-2 and C-3 substituted quinolines and their evaluation as anti-HIV-1 agents, Bioorg. Chem. 80 (2018) 591–601.
[17] P. Gautret, J-C. Lagier, P. Parola, L. Meddeb, M. Mailhe, B. Doudier, Hydroxychloroquine and azithromycin as a treatment of COVID-19: results of an open-label non-randomized clinical trial, Int. J. Antimicrob Agents. 56 (2020) 105–949.
[18] K.M. Kacprzak, Chemistry and biology of cinchona alkaloids, Nat. Prod. (2013) 605–641.
[19] M.E. Wall, M.C. Wani, C.E. Cook, K.H. Palmer, A.T. McPhail, G.A. Sim, Plant antitumor agents I. The isolation and structure of camptothecin, a novel alkaloidal leukemia and tumor inhabitor from *Camptotheca acuminate*, J. Am. Chem. Soc. 88 (1966) 3888–3890.
[20] M.C. Otto, N. Brahma, T. Brain, A versatile new synthesis of quinolines and related fused pyridines, Part 5. The synthesis of 2-chloroquinoline-3-carbaldehydes, J. Chem. Soc., Perkin Trans. 1. (1981) 1520–1530.
[21] V. Nadaraj, S.Thamarai Selvi, The effective reaction of 2-chloro-3-formylquinoline and acetic acid/sodium acetate under microwave irradiation, Int. J. Eng. Res. Technol. 3 (2011) 297–302.
[22] R. D. Dennington, T. A. Keith, J. M. Millam, GaussView 5.0.8, Gaussian Inc (2008).
[23] T. Tsuneda, J.-W. Song, S. Suzuki, K. Hirao, On Koopmans' theorem in density functional theory, J. Chem. Phys. 133 (2010), 174101.
[24] R.G. Parr, R.G. Pearson, Absolute hardness : companion parameter to absolute electronegativity, J. Am. Chem. Soc. 105 (1983) 7512–7516.
[25] R.G. Parr, R.A. Donnelly, M. Levy, W.E. Palke, Electronegativity-the density functional viewpoint, J. Chem. Phys. 68 (1978) 3801–3808.
[26] N. Celikel, G. Kavas, Antimicrobial properties of some essential oils against some pathogenic microorganisms, Czech J. Food Sci. 26 (2008) 174–181.
[27] M. Carcelli, P. Mazza, C. Pelizzi, G. Pelizzi, F. Zani, Antimicrobial and genotoxic activity of 2,6-diacetylpyridine bis(acylhydrazones) and their complexes with some first transition series metal ions. X-ray crystal structure of a dinuclear copper(II) complex, J. Inorg. Biochem. 57 (1995) 43–62.
[28] S. Fengxiang, S. Nannan, S. Fei, Z. Zhiyong, S. Jie, L. Hongzhou, L. Yun, J. Yebin, S. Yuxin, Emerging 2019 novel coronavirus (2019-nCoV) pneumonia, Radiology 25 (2020) 200–274.

[29] Z. Jin, X. Du, Y. Xu, Y. Deng, M. Liu, Y. Zhao, B. Zhang, X. Li, L. Zhang, C. Peng, Y. Duan, J. Yu, L. Wang, K. Yang, F. Liu, R. Jiang, X. Yang, T. You, X. Liu, X. Yang, F. Bai, H. Liu, X. Liu, L.W. Guddat, W. Xu, G. Xiao, C. Qin, Z. Shi, H. Jiang, Z. Rao, H. Yang, Structure of M^{pro} from SARS-CoV-2 and discovery of its inhibitors, Nature 582 (2020) 289–293.
[30] E.D. Dincel, E. Gürsoy, T. Yilmaz-Ozden, N. Ulusoy-Güzeldemirci, Antioxidant activity of novel imidazo[2,1-b] thiazole derivatives: design, synthesis, biological evaluation, molecular docking study and in silico ADME prediction, Bioorg. Chem. 103 (2020), 104220.
[31] A. Daina, O. Michielin, V. Zoete, SwissADME: a free web tool to evaluate pharmacokinetics, drug-likeness and medicinal chemistry friendliness of small molecules, Scientific Reports 7 (2017) 42717.
[32] J.J. McKinnon, D. Jayatilaka, M.A. Spackman, Towards quantitative analysis of intermolecular interactions with Hirshfeld surfaces, Chem Commun 37 (2007) 3814–3816.
[33] M.A. Spackman, J.J. McKinnon, Fingerprinting intermolecular interactions in molecular crystals, Cryst. Eng. Comm. 4 (2002) 378–392.
[34] M. Lamsayah, M. Khoutoul, A. Takfaoui, R. Touzani, High liquid – liquid extraction selectivity of Fe (II) and Pb (II) with TD-DFT theoretical calculations of long chain acid pyrazole- and triazole-based ligands, Cogent Chem 2 (2016) 1–16.
[35] P. Politzer, J.S. Murray, The fundamental nature and role of the electrostatic potential in atoms and molecules, Theor. Chem. Acc. 108 (2002) 134–142.
[36] A.K. Singh, A. Singh, A. Shaikh, R. Singh, A. Misra, Chloroquine and hydroxychloroquine in the treatment of COVID-19 with or without diabetes: a systematic search and a narrative review with a special reference to India and other developing countries, Diabetes Metab. Syndr. 14 (2020) 241–246.
[37] A.S. Achutha, V.L. Pushpa, S. Suchitra, Theoretical insights into the anti-SARS-CoV-2 activity of chloroquine and its analogs and in silico screening of main protease inhibitors, J. Proteome Res. 19 (2020) 4706–4717.
[38] J. Lakshmipraba, S. Arunachalam, R.V. Solomon, P. Venuvanalingam, A. Riyasdeen, R. Dhivya, M.A. Akbarsha, Surfactant–copper (II) Schiff base complexes : synthesis, structural investigation, DNA interaction, docking studies, and cytotoxic activity, J. Biomol. Struct. Dyn. 33 (2015) 877–891.